PAPER *Special Section on Medical Information Communication Technology for Disaster Recovery and Human Health Care Support*

Small Multi-Band Antenna with Tuning Function for Body-Centric Wireless Communications

Chia-Hsien LIN[†a)], ***Student Member***, **Zhengyi LI**[††*], ***Nonmember***, **Kazuyuki SAITO**[††], ***Member***, **Masaharu TAKAHASHI**[††], ***Senior Member***, ***and*** **Koichi ITO**[†], ***Fellow***

SUMMARY The research on body-centric wireless communications (BCWCs) is becoming very hot because of numerous applications, especially the application of E-health systems. Therefore, a small multi-band and low-profile planar inverted-F antenna (PIFA) with tuning function is presented for BCWCs in this paper. In order to achieve multi-band operation, there are two branches in the antenna: the longer branch low frequency band (950–956 MHz), and the shorter branch with a varactor diode embedded for high frequency bands. By supplying different DC voltages, the capacitance of the varactor diode varies, so the resonant frequency can be tuned without changing the dimension of the antenna. While the bias is set at 6 V and 14 V, WiMAX and ISM bands can be covered, respectively. From the radiation patterns, at 950 MHz, the proposed antenna is suitable for on-body communications, and in WiMAX and ISM bands, they are suitable for both on-body and off-body communications.
key words: *body-centric wireless communications (BCWCs), planar inverted-F antenna (PIFA), industrial-scientific-medical (ISM), WiMAX*

1. Introduction

In recent years, the research on body-centric wireless communications (BCWCs) is becoming very hot, because of numerous applications, such as, E-health systems, security agencies, and personal entertainment [1]–[4]. Especially, many researchers considered E-health systems as the biggest potential application with all kinds of wireless devices. In fact, due to population aging, this application will play a more significant part in Japanese society than that in other countries [2], [3]. Therefore, as an interface between the wireless devices and the propagation environment, antennas for BCWCs need to be carefully designed.

At present, some antenna designs have been introduced for BCWCs [5]–[9]. The well-known requirements for wearable antennas in body-centric wireless communications area are compact size, light weight, low-profile, and lower specific absorption rate (SAR). Planar inverted-F antennas in [5]–[7] are good candidates for BCWCs, but the size of these antennas is large due to the large ground plane. In order to reduce antenna size, authors proposed a cavity slot antenna [8] and a small planar inverted-F antenna with folded ground plane [9] for BCWCs. However, only one operation band (2.45 GHz) was achieved in [8], [9]. Actually, besides 2.45 GHz band, several other bands can also be chosen for BCWCs, such as 950–960 MHz, WiMAX, etc. Thus, the design of dual-band or multi-band antennas is also needed. Although dual-band textile antennas with EBG have been proposed for 2.45 and 5 GHz bands in [10], [11], they are difficult to achieve low frequency operation (950–956 MHz) with the similar structure.

In this paper, we proposed a small multi-band and low-profile planar inverted-F antenna (PIFA) with tuning function for BCWCs. In order to achieve multi-band operation, there are two branches on the radiator: the longer branch low frequency band (950–956 MHz), and the shorter branch with a varactor diode embedded for high frequency bands. By supplying different DC voltages, the capacitance of the varactor diode varies, so the higher resonant frequency can be tuned without changing the dimension of the antenna. As an implementation, a varactor diode of Skyworks (SMV2019-040LF) [12] is adopted in our prototype antenna. With this varactor diode, the prototype antenna can cover ISM band (2.40–2.48 GHz) and WiMAX (2.30–2.40 GHz). The radiation patterns of the proposed antenna in 950 MHz can be applied in on-body communications. Furthermore, the radiation patterns of WiMAX and ISM bands are relatively non-directional and are of no deep nulls in the half-sphere above the arm phantom. Therefore, the proposed antenna can be expected to be applied in on-body and off-body communications.

2. Antenna Design

2.1 Antenna Configuration and Human Phantom

As demonstrated in Fig. 1, our proposed antenna is a planar inverted-F antenna. In the antenna, there are two substrate boards, both with a thickness of 0.8 mm and a relative permittivity of 2.17, and the distance between them is 4.4 mm. As a result, the height of the antenna is 6 mm. The lower substrate board has the area of $40 \times 20\,\text{mm}^2$, and the ground plane is on the bottom layer of it, with the same area. The upper substrate board has the area of $40 \times 15\,\text{mm}^2$, and the radiator is on the top layer of it. In Fig. 1(a) the dash line presents the feeding pin. Figure 1(b) presents the side view of the proposed antenna. Figure 1(c) shows the top view of the radiator. The radiator includes a shorter branch

Manuscript received January 12, 2012.
Manuscript revised April 28, 2012.
[†]The authors are with the Graduate School of Engineering, Chiba University, Chiba-shi, 263-8522 Japan.
[††]The authors are with Research Center for Frontier Medical Engineering, Chiba University, Chiba-shi, 263-8522 Japan.
[*]Presently, with Fujitsu Laboratories Ltd., Kanagawa, 211-8588 Japan.
a) E-mail: lch@graduate.chiba-u.jp
DOI: 10.1587/transcom.E95.B.3074

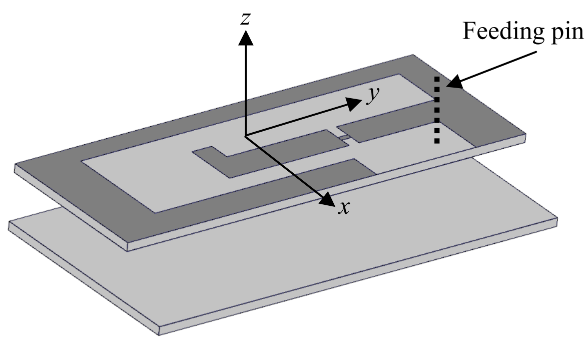

(a) Three-dimensional view

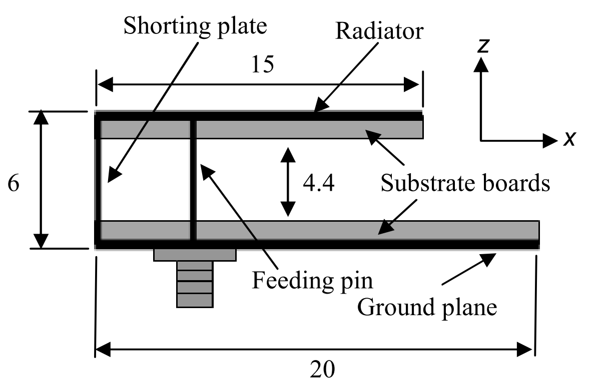

(b) Side view

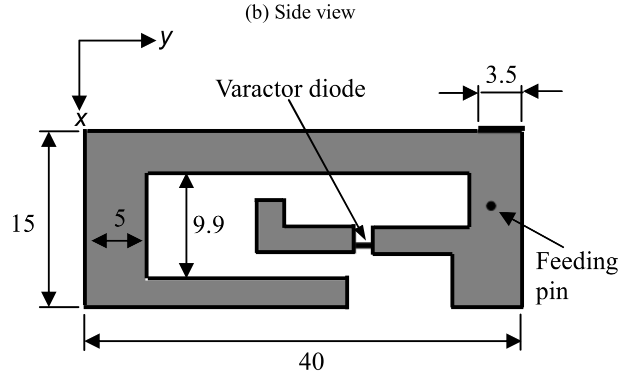

(c) Top view of the radiator

Fig. 1 Structure of the proposed antenna: (a) three-dimensional view, (b) side view and (c) top view of the radiator (unit: mm).

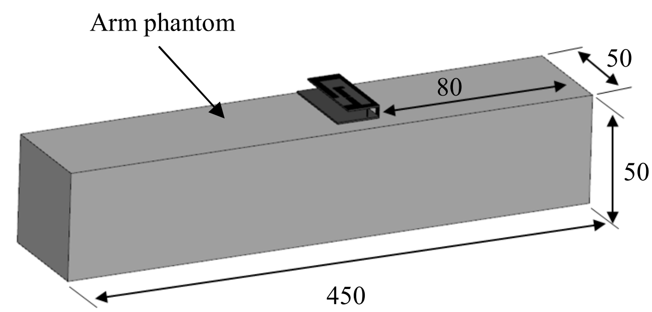

(a) three-dimensional view

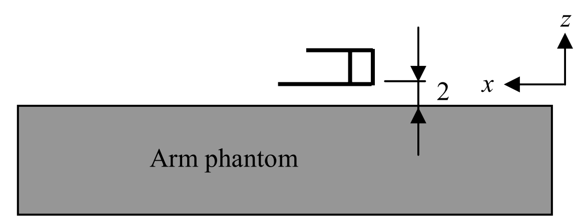

(b) side view

Fig. 2 Antenna and the 2/3 muscle-equivalent phantom: (a) three-dimensional view, and(b) side view (unit: mm).

and a longer branch and one varactor diode is located on the shooter branch as a conducting bridge. By using the two branches and the varactor diode, multi-band operation is achieved. The width of the shorting plate is 3.5 mm. The distance between shorting plate and feeding pin is 5 mm.

Since the proposed antenna is designed for BCWCs, an arm phantom (450 mm × 50 mm × 50 mm) with two-thirds muscle-equivalent electric properties is located close to the antenna. As shown in Fig. 2(a), the antenna is put 80 mm away from the end of the arm phantom, and the distance between the ground plane of the antenna and the surface of the arm phantom is set at 2 mm as shown in Fig. 2(b).

In the beginning of simulation, we investigated three electric properties of the arm phantom at 950 MHz, 2.35, and 2.45 GHz, respectively (relative permittivity, 37.2 at 950 MHz, 35.8 at 2.35 GHz, and 35.2 at 2.45 GHz; conductivity, 0.65 S/m at 950 MHz, 1.15 S/m at 2.35 GHz, and 1.16 S/m at 2.45 GHz [13]). However, it is found that though the three electrical properties of the arm phantom are different, the simulated reflection coefficients are nearly the same. Therefore, in order to save the calculation time, we adopted only one kind of arm phantom (relative permittivity, 35.2; conductivity, 1.16 S/m) in the following simulation.

2.2 Parameter Analysis and Optimization

In order to optimize the proposed antenna, the parametric analysis was performed in this part, by using High-Frequency Structure Simulator (HFSS) 10.1 (Ansoft Corp.). As shown in Fig. 3(a), four key parameters, G, H, W, and S, were analyzed and discussed. Though we used a lumped capacitor with different capacitances to mode the varactor diode, we only used 0 pF (open circuit) in this step for simplicity.

G: By varying the parameter of $G$from 8 mm to 12 mm, the length of the longer branch can be changed. From Fig. 3(b), both the two resonant frequencies shift to higher band, The shift of higher resonant frequency is caused by coupling between the two resonant frequencies.

H: The height of the antenna is also an important parameter. By changing it 5.6 mm to 9.6 mm, the higher resonant frequency shifts down from 2.84 GHz to 2.58 GHz, and the lower frequency shifts up from 0.91 GHz to 0.97 GHz, as shown in Fig. 3(c).

W: Fig. 3(d) presents the simulated reflection coeffi-

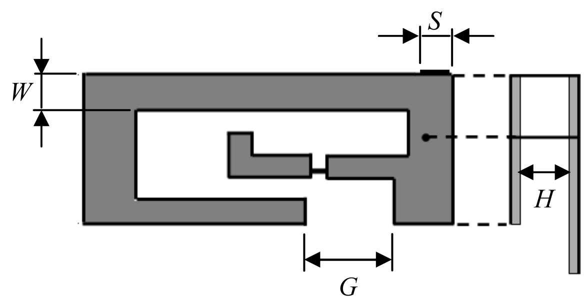

(a) four key parameters

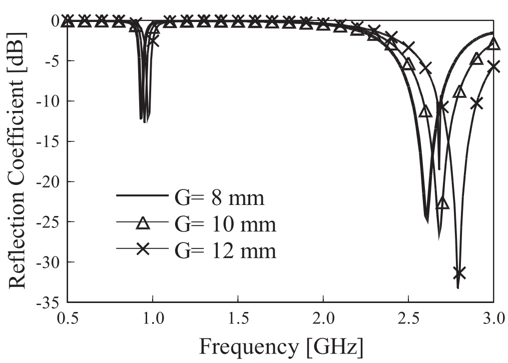

(b) parameter G

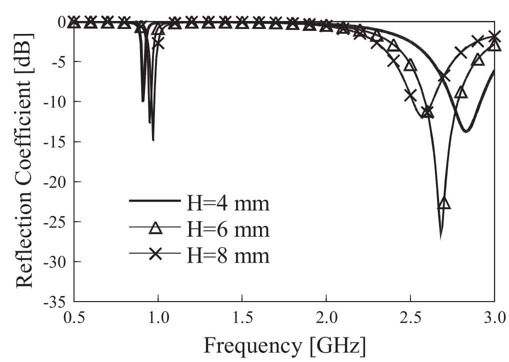

(c) parameter H

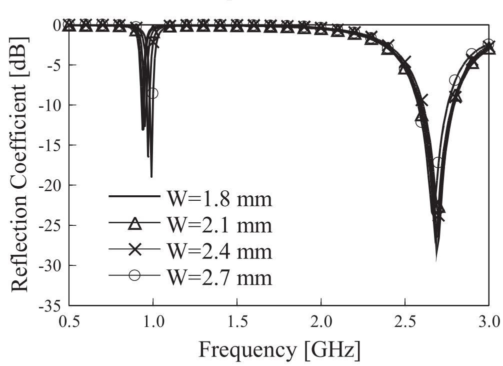

(d) parameter W

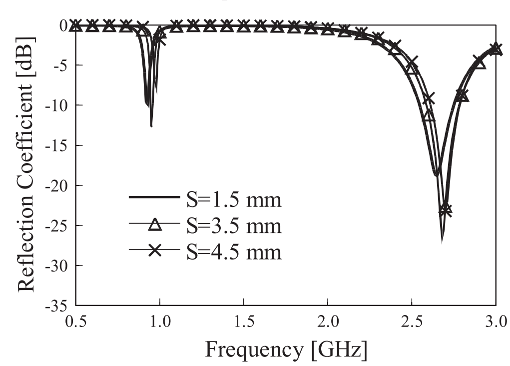

(e) parameter S

Fig. 3 Parametric studies of main radiating element: (a) four key parameters, (b) G, (c) H, (d) W, and (e) S.

cients by increasing the parameter of W. From the results, it does not affect the higher band but make the lower band shift upward from 0.94 GHz to 0.99 GHz because the average current path of longer branch is shortened.

S: By enlarging the width of the shorting plate (S) from 1.5 mm to 4.5 mm the two bands both shift upward, as shown in Fig. 3(e).

Base on the parametric study, the optimized antenna was acquired (G = 10 mm, H= 6 mm, W= 2.1 mm and S= 3.5 mm), and Fig. 4 shows the simulated reflection coefficients. It is found that if the capacitance of the varactor diode increases the higher resonant frequency shifts downward. When the capacitance is set at 0.18 pF, the proposed antenna operates in the ISM band (2.40–2.48 GHz), and when the capacitance is set at 0.27 pF, it operates in the WiMAX band (2.30–2.40 GHz). From the results, the lower

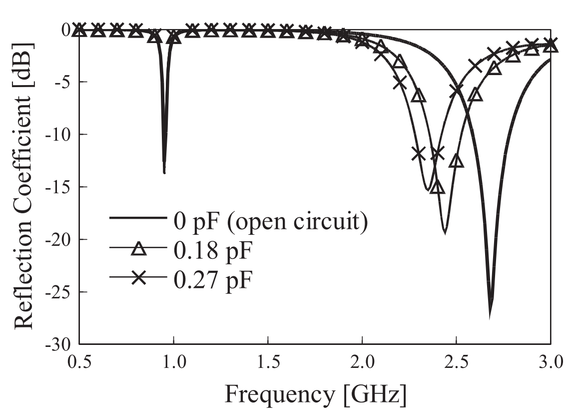

Fig. 4 Simulated reflection coefficient.

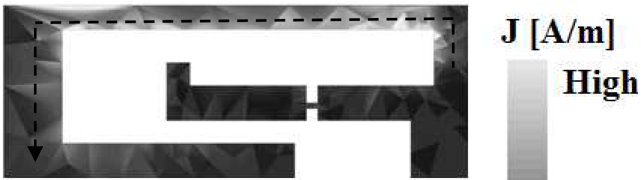

(a) 950 MHz

(b) 2.35 GHz

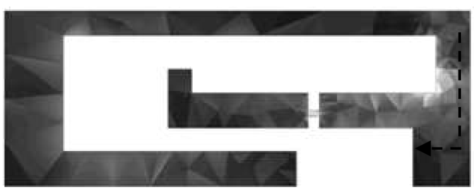

(c) 2.45 GHz

Fig. 5 Simulated surface currents distribution at (a) 950 MHz, (b) 2.35 GHz and (c) 2.45 GHz.

band (950–956 MHz) is also covered.

To understand the multi-band operation of the proposed antenna, the surface current distributions on the radiator at 950 MHz, 2.35 and 2.45 GHz, were given in Fig. 5. As shown in Fig. 5(a), the surface current flows from the feeding point to the end of the longer branch, whose path length is close to one quarter-wavelength of 950 MHz. Figure (b) and (c) show the surface currents flow from the feeding point to the end of the shorter branch, whose path length is close to one quarter-wavelength of 2.4 GHz.

3. Experimental Results and Discussion

3.1 Reflection Coefficients

As an implementation, a varactor diode of Skyworks (SMV2019-040LF) is adopted in our prototype antenna. Besides, as in Fig. 6, two RF chock inductors with 33 nH are added to separate the DC signal and the RF signal. Based on its data sheet [10], a typical characteristic of capacitance is given in Fig. 7, so the varactor diode offers a tuning range of capacitance from 2.10 pF to 0.23 pF over a DC voltage from 0 V to 20 V. It should be noted that, in order to reduce the effects of DC lines, the DC lines are run through two holes both dug on the two substrate boards, as shown in Fig. 8. The arm phantom in our paper is shown in Fig. 9. In our experiment, we dug a hole in the phantom for the connecting cable to the antenna. The arm phantom is comprised of deionized water, agar, sodium chloride, polyethylene powder, TX-151, and sodium dehydroacetic acid [14]. In the measurement, a foam layer with a thickness of 2 mm is used to fix the distance between the antenna and the arm phantom.

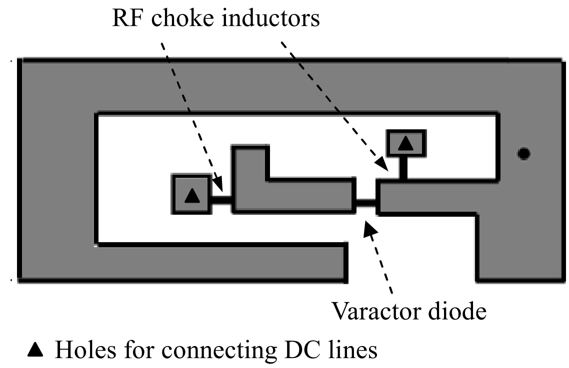

Fig. 6 Layout of the tuning circuit.

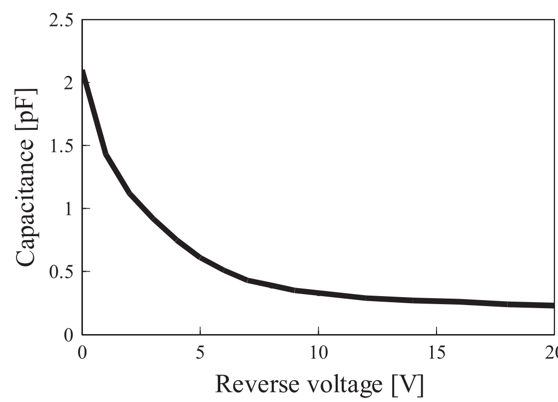

Fig. 7 Capacitance vs reverse voltage.

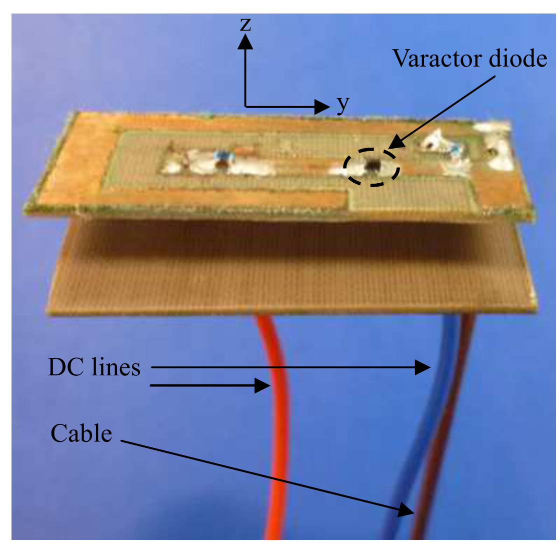

Fig. 8 Prototype antenna.

Figures 10(a) and (b) present the measured reflection coefficients of the proposed antenna with the arm phantom at different bias voltages (6 V and 14 V). From the figures,

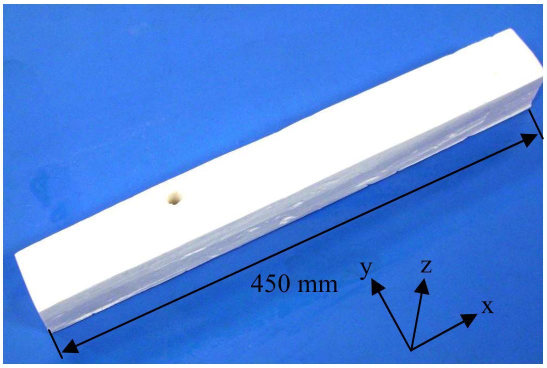

Fig. 9 The proposed 2/3 muscle-equivalent phantom.

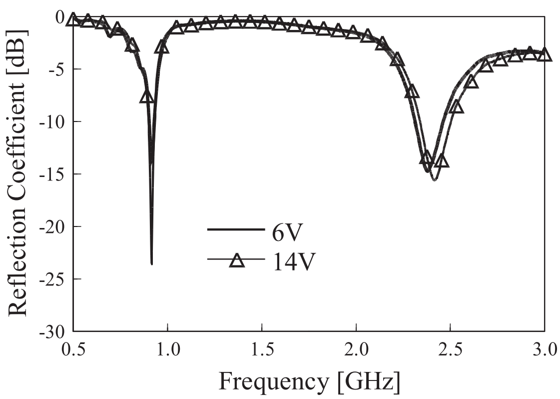

(a)

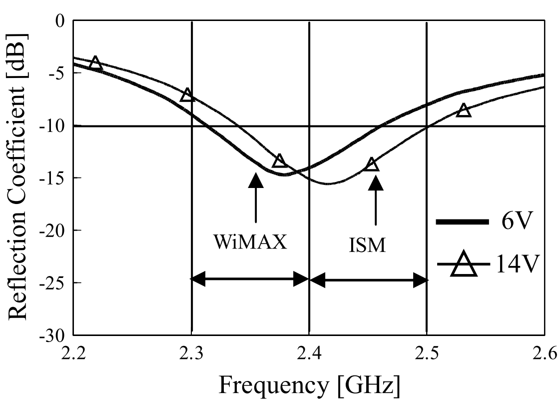

(b)

Fig. 10 Measured reflection coefficients (a) 0.5–3 GHz and (b) 2.2–2.6 GHz.

firstly, the first resonance frequency shifts slightly while the bias voltage is changed; secondly, the second resonance frequency occurs from 2.27 to 2.50 GHz below −10 dB and the WiMAX (2.30–2.40 GHz) and ISM (2.40–2.48 GHz) can be covered while the bias is set 6 V and 14 V, as show in Fig. 10(b). From the results, by increasing the voltage, the operation frequency band is shifted upward, which is because the capacitance of the varactor diode is reduced.

3.2 Radiation Patterns

Besides reflection coefficients, the far-field radiation patterns of the proposed antenna are also studied. Figure 11 illustrates the measured radiation patterns in the *xz* and *yz* planes at 950 MHz, 2.35 GHz and 2.45 GHz. As a comparison, the simulated radiation patterns are added (0.18 and 0.27 pF). The radiation patterns in WiMAX and ISM bands are relatively non-directional and are of no deep nulls in the half-sphere above the arm phantom with wide beam so the proposed antenna is able to be applied in on-body and off-body communications. For 950 MHz, due to weaken radiation in the direction of 0 degree, it can only be applied in on-body communication. In addition, the measured radiation patterns are close to the simulated ones, though there are some difference due to the coaxial cable and the DC lines.

4. Conclusions

The small multi-band antenna with tuning function for body-centric wireless communications is studied in this paper. It is a planar inverted-F antenna and there are two branches on the radiator: the longer branch low frequency band (950–956 MHz), and the shorter branch with a varactor diode embedded for high frequency bands. By supplying different DC voltages, the capacitance of the varactor diode varies, so the resonant frequency can be tuned without changing the dimension of the antenna. While the bias is set at 6 V and 14 V, WiMAX and ISM bands can be covered, respectively. In addition, the radiation patterns in WiMAX and ISM bands are relatively non-directional and are of no deep nulls in the half-sphere above the arm phantom with wide beam so the proposed antenna is able to be applied in on-body and off-body communications. For 950 MHz, due to weaken radiation in the direction of 0 degree, it can only be applied in on-body communication.

References

[1] P. Hall, "Antennas and propagation for body centric communications," Proc. IET Seminar Antennas and Propagation Body-Centric Wireless Communications, pp.1–4, London, UK, April 2007.

[2] http://www.mict.ynu.ac.jp/index

[3] M. Hamalainen, A. Taparugssanagorn, J. Iinatti, and R. Kohno, "Exploitation of wireless technology in remote care processes," IEICE Trans. Commun., vol.E92-B, no.2, pp.373–378, Feb. 2009.

[4] P. Hall, Y. Hao, and K. Ito, "Guest editorial for the special issue on antennas and propagation on body-centric wireless communications," IEEE Trans. Antennas Propag., vol.57, no.4, pp.834–836, April 2009.

[5] P. Salonen, L. Sydänheimo, M. Keskilammi, and M. Kivikoski, "A small planar inverted-F antenna for wearable applications," Third International Symposium on Wearable Computers, pp.95–100, Oct. 1999.

[6] T.S.P. See and Z.N. Chen, "Effects of human body on performance of wearable PIFAs and RF transmission," IEEE Antennas Propag. Symp., vol.1B, pp.686–689, 2005.

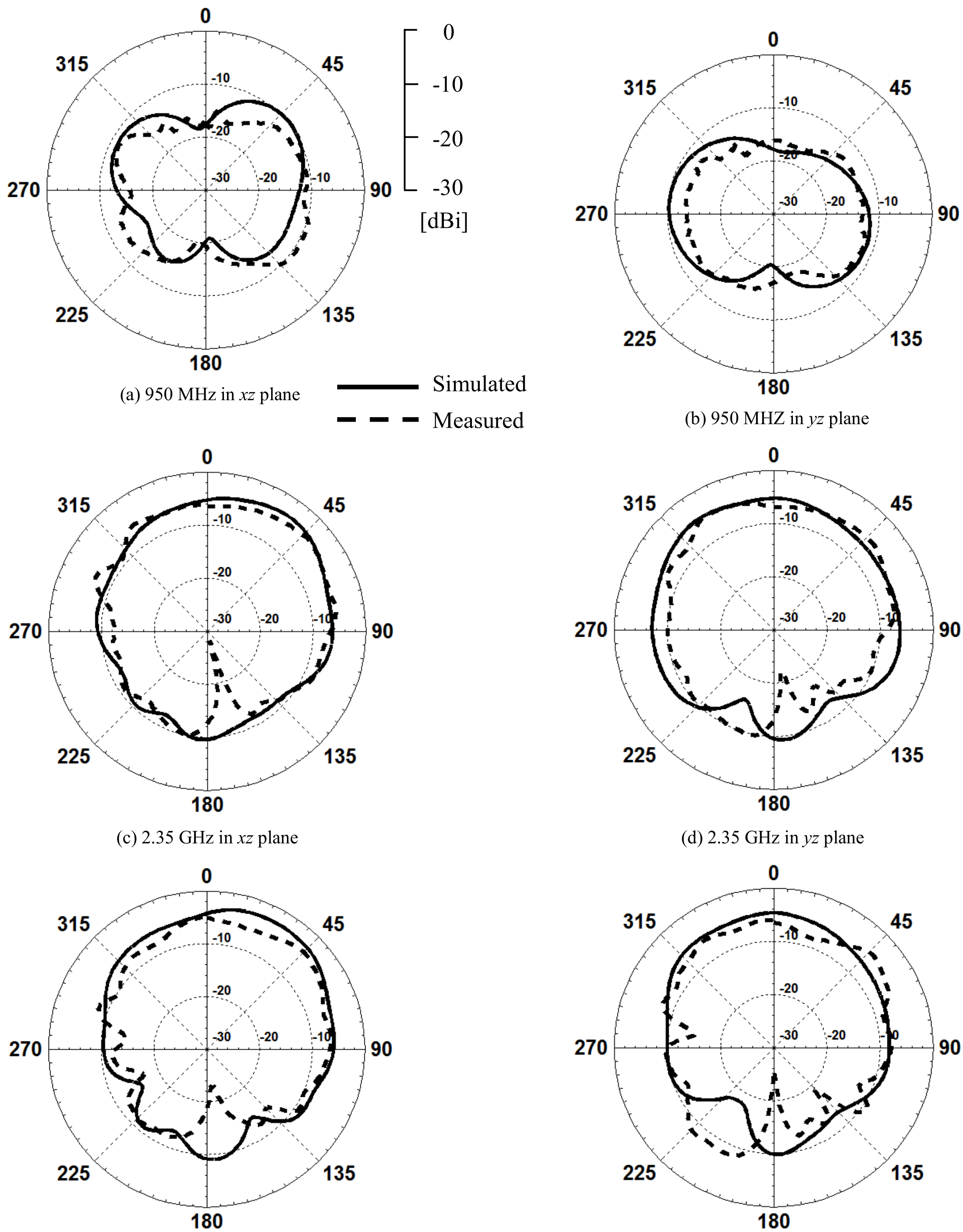

(a) 950 MHz in *xz* plane

(b) 950 MHZ in *yz* plane

(c) 2.35 GHz in *xz* plane

(d) 2.35 GHz in *yz* plane

(e) 2.45 GHz in *xz* plane

(f) 2.45 GHz in *yz* plane

Fig. 11 Simulated and measured radiation patterns (a) at 950 MHz in *xz* plane, (b) at 950 MHZ in *yz* plane, (c) at 2.35 GHz in *xz* plane, (d) at 2.35 GHz in *yz* plane, (e) at 2.45 GHz in *xz* plane, and (f) at 2.45 GHz in *yz* plane (unit: dBi).

[7] P.J. Soh, G.A.E Vandenbosch, V. Volski, and H.M.R Nurul, “Characterization of a simple broadband textile planar inverted-F antenna (PIFA) for on body communications,” ICECom, Croatia, 2010, Sept. 2010.

[8] N. Haga, K. Saito, M. Takahashi, and K. Ito, “Characteristics of cavity slot antenna for body-area networks,” IEEE Trans. Antennas Propag., vol.57, no.4, pp.837–843, April 2009.

[9] Z. Li, K. Saito, M. Takahashi, K. Ito, and Y. Huang, “A small planar inverted-F antenna for body-centric wireless communications,” Proc. Int’ Sym. on Antennas and Propag., pp.1–4, Macau, China, Nov. 2010.

[10] S. Zhu and R. Langley, “Dual-band wearable textile antenna on an EBG substrate,” IEEE Trans. Antennas Propag., vol.57, no.4, pp.926–935, April 2009.

[11] S. Zhu and R. Langley, “Dual-band wearable antennas over EBG substrate,” Electron. Lett., vol.43, no.3, pp.141–142, Feb. 2007.
[12] Data Sheet of SMV2019-040LF varactor diode Application Note [Online]. Available: http://www.skyworksinc.com/
[13] http://transition.fcc.gov/oet/rfsafety/dielectric.html
[14] W. Xie, K. Saito, M. Takahashi, and K. Ito, “Performances of an implanted cavity slot antenna embedded in the human arm,” IEEE Trans. Antennas Propag., vol.57, no.4, pp.837–843, April 2009.

Chia-Hsien Lin was born in Taichung, Taiwan, in October 1983. He received the B.S. degree in electronic engineering from National United University, Maioli, Taiwan, in 2007 and the M.S. in Electrical Engineering from National University of Tainan, Taiwan, in 2009. His main research interests include small antennas for body area network, design of microstrip filters and reconfigurable antennas.

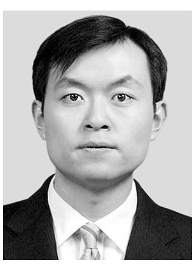

Zhengyi Li was born in Xi’an, China, in February 1982. He received the B.E. degree in Information Engineering from Xi’an Jiaotong University, Xi’an, China, in 2004, and the Ph.D. degree in Electronic Engineering from Tsinghua University, Beijing, China, in 2010. From 2010 to 2012, he was a Postdoctoral Researcher at the Research Center for Frontier Medical Engineering, Chiba University. He is currently a Researcher at Fujitsu Laboratories Ltd. His research interests include small antennas for body-centric wireless communications, MIMO antennas, and reconfigurable antennas. Dr. Li was the recipient of the 2010 Asia-Pacific Radio Science Conference (AP-RASC’10) Young Scientist Award in 2010.

Kazuyuki Saito was born in Nagano, Japan, in May 1973. He received the B.E., M.E. and D.E. degrees all in electronic engineering from Chiba University, Chiba, Japan, in 1996, 1998 and 2001, respectively. He is currently an Associate Professor with the Research Center for Frontier Medical Engineering, Chiba University. His main interest is in the area of medical applications of the microwaves including the microwave hyperthermia. Prof. Saito received the IEICE AP-S Freshman Award, the Award for Young Scientist of URSI General Assembly, the IEEE AP-S Japan Chapter Young Engineer Award, the Young Researchers’ Award of IEICE, and the International Symposium on Antennas and Propagation (ISAP) Paper Award in 1997, 1999, 2000, 2004, and 2005 respectively. Dr. Saito is a member of the Institute of Image Information and Television Engineers of Japan (ITE), and the Japanese Society for Thermal Medicine.

Masaharu Takahashi was born in Chiba, Japan, in December, 1965. He received the B.E. degree in electrical engineering in 1989 from Tohoku University, Miyagi, Japan, and the M.E. and D.E. degrees both in electrical engineering from Tokyo Institute of Technology, Tokyo, Japan, in 1991 and 1994 respectively. He was a Research Associate from 1994 to 1996, an Assistant Professor from 1996 to 2000 at Musashi Institute of Technology, Tokyo, Japan, and an Associate Professor from 2000 to 2004 at Tokyo University of Agriculture and Technology, Tokyo, Japan. He is currently an Associate Professor at the Research Center for Frontier Medical Engineering, Chiba University, Chiba, Japan. His main interests are electrically small antennas, planar array antennas, and electromagnetic compatibility. Prof. Takahashi received the IEEE Antennas and Propagation Society (IEEE AP-S) Tokyo chapter young engineer award in 1994.

Koichi Ito was born in Nagoya, in June, 1950. He received the B.S. and M.S. degrees from Chiba University, Chiba, Japan, in 1974 and 1976, respectively, and the D.E. degree from the Tokyo Institute of Technology, Tokyo, Japan, in 1985, all in electrical engineering. From 1976 to 1979, he was a Research Associate at the Tokyo Institute of Technology. From 1979 to 1989, he was a Research Associate at Chiba University. From 1989 to 1997, he was an Associate Professor at the Department of Electrical and Electronics Engineering, Chiba University, and is currently a Professor at the Graduate School of Engineering, Chiba University. He has been appointed as one of the Deputy Vice-Presidents for Research, Chiba University, since April 2005. In 1989, 1994, and 1998, he visited the University of Rennes I, France, as an Invited Professor. Since 2004 he has been appointed as an Adjunct Professor to Institute of Technology Bandung (ITB), Indonesia. His main research interests include analysis and design of printed antennas and small antennas for mobile communications, research on evaluation of the interaction between electromagnetic fields and the human body by use of numerical and experimental phantoms, microwave antennas for medical applications such as cancer treatment, and antennas for body-centric wireless communications. Dr. Ito is a member of the American Association for the Advancement of Science, the Institute of Image Information and Television Engineers of Japan (ITE) and the Japanese Society for Thermal Medicine (formerly, Japanese Society of Hyperthermic Oncology). He served as Chair of the Technical Group on Radio and Optical Transmissions, ITE from 1997 to 2001 and Chair of the Technical Group on Human Phantoms for Electromagnetics, IEICE from 1998 to 2006. He also served as Chair of the IEEE AP-S Japan Chapter from 2001 to 2002 and TPC Co-Chair of the 2006 IEEE International Workshop on Antenna Technology (iWAT2006). He currently serves as General Chair of the iWAT2008 to be held in Chiba, Japan in 2008, Vice-Chair of the 2008 International Symposium on Antennas and Propagation (ISAP2008) to be held in Taiwan in 2008 and as an Associate Editor for the IEEE TRANSACTIONS ON ANTENNAS AND PROPAGATION. He also serves as a Distinguished Lecturer and an AdCom member for the IEEE Antennas and Propagation Society since January 2007.